J. Fluid Mech. (1987), *vol.* 183, *pp.* 123–146
Printed in Great Britain

A linear analysis of rotating stratified flow past a circular cylinder on a β-plane

By LEE-OR MERKINE

Department of Mathematics, Technion – Israel Institute of Technology, Haifa 32000, Israel

(Received 26 May 1985 and in revised form 17 February 1987)

A linear analysis of rotating stratified quasi-geostrophic flow past a circular cylinder on a β-plane is performed for moderate stratification, i.e. for $\sigma S = O(E^{\frac{1}{3}})$, covering effectively the range $E^{\frac{2}{3}} \ll \sigma S \ll 1$, and for strong stratification such that $\sigma S = O(1)$. $E \ll 1$ is the Ekman number and σS is the product of the Prandtl number and the inverse rotational Froude number. The parameter β measures the importance of the production of relative vorticity by meridional motion. The analysis pivots about a range of β which constrains the interior motion to follow geostrophic contours. For moderate stratification $\beta = O(E^{\frac{1}{3}})$, covering effectively the range $E^{\frac{1}{3}} \ll \beta \ll E^{\frac{1}{6}}$, while for strong stratification $E \ll \beta \ll 1$. The dominance of β in the interior is responsible for creating a narrow intense boundary layer along the eastern sector of the cylinder and an extensive blocked flow region surrounded by intense free shear layers west of the cylinder. These narrow regions which channel horizontally $O(1)$ mass flux communicate through corner-like regions centred about the extreme meridional locations of the cylinder. The effect of stratification is to shear the flow vertically and to induce counter-flows laterally. When the stratification is strong the z-dependence is parametric. Nonlinear effects can be ignored when the Rossby number, ϵ, satisfies the constraints $\epsilon \ll E^{\frac{11}{12}}$ for moderate stratification and $\epsilon \ll \beta^{\frac{1}{2}} E^{\frac{5}{6}}$ for strong stratification. When expressed in terms of the Reynolds number, $Re = \epsilon/E$, smallness of nonlinear effects can be assured also for high-Reynolds-number flows.

1. Introduction

The experimental work of Boyer (1970) of flow past a circular cylinder in a rotating system on an f-plane led the way to an intensive investigation of the general problem of flow separation in such systems. The experiments demonstrated that sufficiently small Rossby numbers could delay the onset of separation for Reynolds numbers well above the critical value obtained for non-rotating systems. Using the quasi-geostrophic approximation Walker & Stewartson (1972) derived a criterion for flow separation, which is expressed as a ratio of the Rossby number, ϵ, to the square root of the Ekman number, E. Merkine & Solan (1979) used a different formulation to account for certain asymmetries observed in Boyer's experiments but obtained the same criterion for separation as Walker & Stewartson.

Additional and more refined experiments were conducted by Boyer & Davies (1982) who emphasized β-plane effects measured by the parameter β. The experiments which were conducted in the parameter regime $E^{\frac{1}{3}} = O(\epsilon), \beta = O(\epsilon)$ showed that β inhibits separation in prograde flows but enhances it in retrograde flows. (The exact definition of ϵ, E and β all of which are assumed small, is given in the next section.) The experiments confirmed the boundary-layer analysis of Merkine (1980) predicting that separation is inhibited by β in prograde flows. Yet, the parameter regime of that

study did not quite apply to the experiments since spin-down of vorticity was neglected compared to diffusion of vorticity. In a recent study of flow separation in a two-layer rotating fluid, Merkine & Brevdo (1986) considered also the parameter regime of Boyer & Davies (1982). Using boundary-layer techniques they were able to obtain better agreement with the results of Boyer & Davies for both prograde and retrograde flows. The vertical boundary-layer structure was still that of Stewartson, namely the $E^{\frac{1}{4}}$ and $E^{\frac{1}{3}}$ layers but the interior tangential velocity impressed on it was a function of $E^{\frac{1}{2}}\epsilon, \beta/\epsilon$ and the flow direction at infinity.

Figure 5 of Boyer & Davies (1982) shows that both prograde and retrograde flows exhibit divergence of streamlines west of the cylinder and convergence of streamlines east of it. (North is defined as the direction of increasing basic rotation.) These effects were accentuated in the nonlinear analytic study of Foster (1985) who considered, for prograde flows only, the parameter range $E^{\frac{1}{2}} \ll \beta \ll E^{\frac{1}{4}}$. In this range of β the western divergence becomes an extensive blocked region surrounded by free shear layers and the eastern convergence evolves into a narrow layer with very high velocities adjacent to the eastern sector of the cylinder. This latter layer was referred to by Foster as the Rossby layer. (These features are discussed also in Merkine & Brevdo (1986) for $\beta = O(E^{\frac{1}{2}})$.) Foster showed also that separation is delayed until the boundary layer attains a much higher level of nonlinearity. To be more specific, in the parameter regime of the experiments the $E^{\frac{1}{4}}$ layer becomes nonlinear when $\epsilon/E^{\frac{1}{2}} = O(1)$ and the criterion for separation is given by $\epsilon/E^{\frac{1}{2}} = f(\beta/\epsilon)$ where $f(\beta/\epsilon)$ is of order unity and depends on the flow direction. In Foster's study, however, the $E^{\frac{1}{4}}$ layer in the eastern sector becomes nonlinear when $\epsilon\beta/E = O(1)$, that is at much lower values of ϵ, but separation is delayed to Rossby numbers much larger than E/β. The nonlinear $E^{\frac{1}{4}}$ layer of Foster is still Stewartson-like but it is controlled by a thicker layer of thickness $E^{\frac{1}{2}}/\beta$, the Rossby layer, which carries an $O(1)$ mass flux and whose sructure is such as to delay the separation of the $E^{\frac{1}{4}}$ layer. We observe that the Reynolds number of the flow defined as $Re = \epsilon/E$ can be large even if nonlinear effects are small such that $\epsilon\beta/E \ll 1$. In this case the linear dynamics prevails everywhere but the Rossby layer still channels the $O(1)$ mass flux.

When $\beta = O(E^{\frac{1}{4}})$ the Rossby layer merges with the $E^{\frac{1}{4}}$ layer which is no longer Stewartson-like. It is advantageous to analyse such a layer since for small values of the ratio $\beta/E^{\frac{1}{4}}$ we recover Foster's regime while for large values of the ratio we gain insight into the dynamics that exists when $E^{\frac{1}{4}} \ll \beta \ll E^{\frac{1}{3}}$. (When $\beta = O(E^{\frac{1}{3}})$ the Rossby layer merges with the $E^{\frac{1}{3}}$ layer and its dynamics is no longer quasi-geostrophic.) Such an approach will be taken when stratified fluids are considered later in this work. Summarizing the role of β, we observe that as it increases from zero its effects penetrate from infinity. When $\beta \ll E^{\frac{1}{2}}$ the entire flow field behaves essentially as if it is on an f-plane. When $\beta = O(E^{\frac{1}{2}})$ distinction appears between prograde and retrograde flows in the interior which for prograde flows contains damped Rossby waves. When $\beta \gg E^{\frac{1}{2}}$ we enter Foster's regime. The interior flow is constrained to follow geostrophic contours and β starts to participate directly in the boundary-layer dynamics.

The above studies assumed homogeneous fluids but from the point of view of possible geophysical applications it is of considerable interest to learn how stratification affects separation. It turns out that the degree of complexity introduced by stratification is considerable but it is worth pursuing since new dynamical features are discovered. A linear analysis of rotating continuously stratified flow past a right circular cylinder on an f-plane is given by Merkine (1985). In the present work we extend that study to the β-plane where, as in Foster's study, β is allowed to dominate

the dynamics. Because of the intricacy of the dynamics we find it instructive to recapitulate the major parameter regimes of the stratified f-plane.

Barcilon & Pedlosky (1967*a*, *b*) carried out a most thorough investigation of the linear dynamics of contained rotating stratified fluids. Denoting by σS the stratification parameter where σ is the Prandtl number and S is the inverse of the rotational Froude number (the exact definition of σ and S is given in the next section), Barcilon & Pedlosky concluded that when $\sigma S \ll E^{\frac{4}{3}}$ the fluid behaves as if it were essentially homogeneous while for $\sigma S \gg E^{\frac{1}{2}}$ it is dominated everywhere by stratification. In the intermediate region $E^{\frac{1}{3}} \ll \sigma S \ll E^{\frac{1}{2}}$ the dynamics was found to be of a hybrid nature, exhibiting features of both homogeneous and stratified fluids. As σS increases from zero the effects of stratification are found to penetrate from the vertical wall into the interior. This direction of penetration is in opposite sense to that of β and it follows from the fact that it is the vertical velocity which attains its largest values next to the vertical wall and hence is affected first by the degree of stratification present. In the intermediate region standard Ekman layers are present along the horizontal boundaries and the vertical boundary layer splits into three sublayers which are respectively, the innermost layer of thickness $(\sigma S)^{-\frac{1}{4}}E^{\frac{1}{2}}$, the intermediate hydrostatic baroclinic layer of thickness $(\sigma S)^{\frac{1}{2}}$ and the outer homogeneous layer of thickness $E^{\frac{1}{4}}$. In the strongly stratified limit Ekman layers no longer control the dynamics and, in fact, they are frequently absent. Along the vertical walls only the buoyancy layer, now of thickness $E^{\frac{1}{2}}$, remains.

To capture effectively the effects of stratification when a vertically sheared external flow impinges on a vertical cylinder Merkine (1985) considered two parameter regimes $\sigma S = O(E^{\frac{1}{2}})$ and $\sigma S = O(1)$ which are referred to as the moderate and strong regimes of stratification, respectively. In the first regime the intermediate baroclinic hydrostatic layer merges with the external $E^{\frac{1}{4}}$ homogeneous layer yielding a baroclinic hydrostatic $E^{\frac{1}{4}}$ layer which is in geostrophic balance. The innermost buoyancy layer shrinks to $O(E^{\frac{3}{8}})$. By allowing the ratio $\sigma S/E^{\frac{1}{2}}$ to assume a continuous range of values from small to large it was possible, in the context of external flows, to exhibit in a single formulation how stratification affects the dynamics as it increases from small to moderately strong values. The case of strong stratification was then treated separately. The interior flow was controlled by viscous diffusive processes and for the particular problem considered it could satisfy to leading order all the necessary boundary conditions without necessitating the narrow $E^{\frac{1}{2}}$ vertical buoyancy layer.

The major finding of the linear analysis of Merkine (1985) was that oncoming flows which are of one sign but possess vertical shear can induce flow reversal regions next to the cylinder. Depending on the degree of stratification these regions can occupy the inner part of the vertical boundary layer or can extend horizontally across distances comparable to the horizontal scale of the cylinder. Based on the nonlinear, two-layer, f-plane study of Brevdo & Merkine (1985), which demonstrates the existence of fully attached boundary layers with inner flow reversal regions, Merkine (1985) argued that nonlinearity should push the backflow region downstream of the forward stagnation point and should cause separation to occur at the rear stagnation point. When the stratification is moderate the linear analysis is valid as long as $\epsilon = o(E^{\frac{1}{2}})$ and when the stratification is strong it is valid as long as $\epsilon = o(E)$. Thus, the former case can correspond to high-Reynolds-number flows since the requirement is that $Re = o(E^{-\frac{1}{2}})$, but the latter case is certainly a slow flow problem since $Re = o(1)$ and hence of no direct geophysical applicability. It can apply, however, to laboratory situations. We note that the interior slow flow should not be thought of as a creeping Stokes flow since it is still in geostrophic hydrostatic balance.

We can envision now the role of β when incorporated into the linear analysis of Merkine (1985) and consider moderate stratification first. f-plane dynamics essentially prevails uniformly when $\beta \ll E^{\frac{1}{2}}$. When $\beta = O(E^{\frac{1}{2}})$, β-effects become important in the interior but the boundary layers that exist next to the cylinder still have the f-plane structure. β affects them only through the asymptotic matching condition on the tangential velocity and this situation still prevails when $E^{\frac{1}{2}} \ll \beta \ll E^{\frac{1}{4}}$. Now, however, the interior flow is constrained to follow geostrophic contours and a linear Rossby layer develops next to the cylinder and on top of the $E^{\frac{1}{4}}$ layer. When $\beta = O(E^{\frac{1}{4}})$ the Rossby layer merges with the hydrostatic baroclinic $E^{\frac{1}{4}}$ layer which must now carry $O(1)$ mass flux. Thus it seems interesting physically to consider the two parameter regimes $\beta = O(E^{\frac{1}{2}})$ and $\beta = O(E^{\frac{1}{4}})$ covering effectively the range $0 \leqslant \beta \ll E^{\frac{1}{2}}$. (The upper bound is determined by the buoyancy layer.) It turns out, as explained in the next section, that it is not possible to obtain analytical solutions for the interior flow when $\beta = O(E^{\frac{1}{2}})$. However, Merkine & Brevdo (1986) considered this flow regime including nonlinear effects in the context of a two-layer model for a vertically sheared flow and much physical insight can be gained from that study. Analytical solutions are possible when $\beta = O(E^{\frac{1}{4}})$ and they are discussed in §3. Thus the range of parameters covered in the case of moderate stratification is effectively given by $E^{\frac{1}{2}} \ll \beta \ll E^{\frac{1}{3}}$ and $E^{\frac{2}{3}} \ll \sigma S \ll 1$.

The situation is different when stratification is strong. In the f-plane case the interior vertical velocity is suppressed to $O(E)$ and it is at this order that the geostrophic degeneracy is removed. Thus when $\beta \ll E$ the dynamics is still f-plane-like. But when $\beta = O(E)$, β-effects become as important as the viscous diffusive processes which control the leading-order interior flow. (Recall that this interior flow can satisfy to leading order all the necessary boundary conditions stated in Merkine 1985.) It turns out again, as argued in the next section, that no analytical solutions of the linear problem are possible when $\beta = O(E)$. However, when $E \ll \beta \ll 1$ the interior flow is constrained to follow geostrophic contours and a new boundary layer of thickness $O((E/\beta)^{\frac{1}{3}})$ develops next to the cylinder. (The dynamics of this boundary layer is always quasi-geostrophic by virtue of the smallness of β which ensures that the layer is thicker than $E^{\frac{1}{4}}$.) Linear analysis is possible in this range of β and $\sigma S = O(1)$. It is given in §4.

Foster has shown in his problem that nonlinear effects become important when $\epsilon\beta/E = O(1)$. The linear analysis of the two stratification regimes discussed in the present work, when β is large in the sense stated above, places different constraints on the Rossby number. Because of the considerable complexity of the problem we find it less confusing to assess nonlinear effects as we proceed with the analysis. Suffice it to state here that in the case of moderate stratification nonlinear effects can be ignored as long as $\epsilon \ll E^{\frac{1}{2}}$ and in terms of the Reynolds number the constraint is $Re \ll E^{-\frac{1}{2}}$. It follows that the Reynolds number can still be large. When the stratification is strong nonlinear effects can be ignored as long as $\epsilon \ll E^{\frac{4}{7}}\beta^{\frac{1}{7}}$ and the corresponding constraint on the Reynolds number is $Re \ll \beta^{\frac{1}{7}}/E^{\frac{1}{7}}$ which can also be large. This is a surprising result since in the corresponding f-plane case the Reynolds number is constrained to be small. In spite of the considerable difference in the parameter regimes between the linear version of Foster's problem and the present work we find the same basic structure which is, however, sheared vertically as a consequence of stratification.

2. Formulation

We consider an incompressible, viscous, heat-conducting fluid confined between two horizontal planes at distance D apart. The system is on a β-plane such that it rotates about the vertical z-axis with an angular velocity Ω which varies linearly with $y, \Omega = \Omega_0 + \beta^* Dy$. The y-axis corresponds to the meridional direction of geophysical flows. A horizontally uniform vertically sheared flow with characteristic velocity V is forced in the x-direction past a vertical cylinder of radius $r_0 D$ which extends throughout the depth of the system. Using V and D as reference scales we obtain for steady motions the following linearized non-dimensional equations

$$(1+\beta y)\,\hat{\boldsymbol{k}} \times \boldsymbol{q} = -\nabla_{\mathrm{H}} P + \tfrac{1}{2}E\nabla^2 \boldsymbol{q}, \tag{2.1}$$

$$0 = -P_z + T + \tfrac{1}{2}E\nabla^2 w, \tag{2.2}$$

$$\nabla_{\mathrm{H}} \cdot \boldsymbol{q} + w_z = 0, \tag{2.3}$$

$$\sigma S w = \tfrac{1}{2}E\nabla^2 T. \tag{2.4}$$

$\boldsymbol{q}$ is the horizontal velocity vector and w is the vertical component of velocity. Horizontal two-dimensional operators are denoted by the subscript H. The dynamic pressure and temperature are denoted by P and T, respectively. The ratio of the kinematic viscosity, ν, to the heat conductivity, k, is defined by the Prandtl number σ. $E = \nu/\Omega_0 D^2$ is the Ekman number and $S = \alpha \Delta T g/4\Omega_0^2 D$ is the rotational stratification parameter. g is the acceleration of free fall and α is the coefficient of thermal expansion. $\Delta T \geqslant 0$ is the basic temperature difference of the equilibrium state and it is assumed that $\alpha \Delta T \ll 1$. $\beta = \beta^* D/\Omega_0$ is the β-parameter.

Equations (2.1)–(2.4) are supplemented by the boundary conditions

$$\boldsymbol{q} = w = 0, \quad \boldsymbol{n} \cdot \nabla T = 0 \quad \text{on } z = 0, 1 \quad \text{and } r = r_0 \tag{2.5}$$

and

$$P = \mp[a + b(z - \tfrac{1}{2})]\, y \quad \text{as } r \to \infty. \tag{2.6}$$

a and b are positive constants and (2.6) implies that at large distances from the cylinder the motion is in exact geostrophic balance and can be either prograde or retrograde provided that $2a - b > 0$. The condition of no heat flux imposed on the dynamical part of the temperature field simplifies the analysis (Barcilon & Pedlosky 1967*b*) and allows direct comparison of the theory with laboratory experiments which utilize salinity rather than temperature as the agent of stratification (Boyer *et al.* 1987).

The f-plane dynamics discussed by Merkine (1985) is governed by (2.1)–(2.6) with $\beta = 0$. Following that work our analysis pivots on the parameter constraint $E \ll 1$ such that the system is moderately stratified when $\sigma S = O(E^{\frac{1}{2}})$ or strongly stratified when $\sigma S = O(1)$. It is assumed also that $\beta \ll 1$ but it is the relative magnitude of β and E which determines the importance of the β-effect. When the latter operates on the dynamical level set by E and S, such that $\beta = O(E^{\frac{1}{2}})$ when the system is moderately stratified and $\beta = O(E)$ when it is strongly stratified, decaying Rossby waves fill the interior. The leading-order pressure field, P^0, in each of these two cases is governed in the linear regime by the potential vorticity equation $\nabla^2 P^0_{zz} = (2\sigma S\beta/E)\, P^0_x$ for moderate stratification and by

$$\nabla^2\left(\nabla_{\mathrm{H}}^2 + \frac{1}{\sigma S}\frac{\partial^2}{\partial z^2}\right) P^0 = (2\beta/E)\, P^0_x$$

for strong stratification, subject to appropriate boundary conditions. The boundary-value problem thus obtained is intractable analytically. In the strong stratification case, for example, the coefficient of each vertical eigenfunction can be written as

$$\sum_{n=1}^{\infty} G_n(r) \sin n\theta$$

where r and θ are the polar coordinates and G_n are governed by an infinite system of fourth-order coupled ordinary differential equations with modified-Bessel-function-like properties. It turns out that an analytical approach is possible and significant physical understanding can be obtained when β is sufficiently strong such that the interior motion is constrained to follow geostrophic contours. Following the lengthy discussion of the previous section we require that $\beta = O(E^{\frac{1}{4}})$ when the stratification is moderate and that $E \ll \beta \ll 1$ when the stratification is strong. Nonlinear effects can be neglected if we assume that the Rossby number, defined as $\epsilon = V/2\Omega_0 D$, satisfies the constraints stated at the end of the previous section.

3. Strong β, moderate stratification, $\beta = O(E^{\frac{1}{4}}), \sigma S = O(E^{\frac{1}{2}})$

It is shown in Barcilon & Pedlosky (1967*a*) that even for σS as large as $O(1)$ the dynamics of the Ekman layers are not affected by stratification. Consequently the standard Ekman suction condition $w = \pm\frac{1}{2}E^{\frac{1}{2}}\zeta, z = \frac{1}{2}\mp\frac{1}{2}$ can be used where ζ is the leading-order vertical component of the relative vorticity. This $O(E^{\frac{1}{2}})$ estimate of the vertical velocity is consistent with the estimate derived from the temperature equation (2.4) when the stratification is moderate. It follows that outside sharp gradient regions the following expansion of the field variables seems appropriate

$$\left.\begin{aligned} P = P^0 + E^{\frac{1}{4}}P^1 + \ldots, \quad q = q^0 + E^{\frac{1}{4}}q^1 + \ldots, \\ T = T^0 + E^{\frac{1}{4}}T^1 + \ldots, \quad w = E^{\frac{1}{2}}w^0 + \ldots. \end{aligned}\right\} \tag{3.1}$$

Substitution of (3.1) into (2.1)–(2.4) yields the following geostrophic hydrostatic balance for the leading-order motion:

$$\left.\begin{aligned} q^0 &= \hat{k} \times \nabla P^0, \\ T^0 &= P^0_z. \end{aligned}\right\} \tag{3.2}$$

Since $\beta = O(E^{\frac{1}{4}})$, the $O(E^{\frac{1}{4}})$ vorticity equation restricts the leading-order horizontal motion to following geostrophic contours and we obtain

$$v^0 = \frac{\partial P^0}{\partial x} = 0 \Rightarrow P^0 = P^0(y, z), \tag{3.3}$$

where v^0 is the meridional velocity.

It is obvious that the geometric constraint imposed by the cylinder requires lateral motion of at least that portion of the flow field that lies in the range $-r_0 < y < r_0$. The conflict between this requirement and (3.3) can be resolved in several ways. One possibility requires that the lateral deflection of fluid particles takes place over distances which are much larger than r_0. This slow lateral deflection must be accompanied by a blocked region in the vicinity of the cylinder and in this region u, the x-component of velocity, must be small. The other possibility requires the existence of a vertical boundary layer next to the cylinder which is capable of deflecting around it an $O(1)$ mass flux.

Foster (1985) showed that the two possibilities exist in different parts of the flow

domain when homogeneous flow is considered. A blocked region exists to the west of the cylinder while a narrow boundary-layer is adjacent to it in the east. The two regions exchange the $O(1)$ mass flux through a singular rectangular corner region located on the cylinder at $y = \pm r_0$. The transition between the weak blocked flow west of the cylinder and the unblocked unidirectional flow that exists for $|y| > r_0$ occurs in a narrow free shear layer which commences at the corner region and spreads laterally away from it. Our study shows that this basic structure prevails also when the fluid is stratified. The details depend, of course, on the degree of stratification. In the rest of the flow field the pressure distribution (2.6) holds to leading order.

3.1. *The deflecting vertical layer*

The study of Merkine (1985), which is based on the earlier considerations of Barcilon & Pedlosky (1967*b*), shows that for moderate stratification and in the f-plane case the vertical boundary layer along the cylinder consists of two sublayers. The thicker $E^{\frac{1}{4}}$ layer is necessary for imposing the wall conditions on the leading-order horizontal motion and temperature field. The inner $E^{\frac{3}{8}}$ layer is required for applying the no-slip condition to the leading-order vertical velocity. The same boundary layer splitting exists here but now the $E^{\frac{1}{4}}$ layer must also deflect around the cylinder an $O(1)$ mass flux. We denote by u_r and u_θ the radial and tangential velocity components and rescale the $E^{\frac{1}{4}}$ layer variables as follows:

$$\left.\begin{aligned} \rho &= (r-r_0)/E^{\frac{1}{4}}, \\ P &= \tilde{P}, \\ u_r &= \tilde{u}_r, \\ u_\theta &= \tilde{u}_\theta/E^{\frac{1}{4}}, \\ w &= \tilde{w}, \\ T &= \tilde{T}. \end{aligned}\right\} \tag{3.4}$$

All the tilde variables are $O(1)$ as $E \to 0$. Substitution of (3.4) into (2.1)–(2.4) shows that the leading-order motion is in the geostrophic hydrostatic balance

$$\tilde{u}_\theta = \frac{\partial \tilde{P}}{\partial \rho}, \quad \tilde{u}_r = -\frac{1}{r_0}\frac{\partial \tilde{P}}{\partial \theta}, \quad \tilde{T} = \tilde{P}_z. \tag{3.5}$$

Eliminating the vertical velocity from the vertical component of the vorticity equation, using the temperature equation, leads to the following leading-order potential-vorticity equation

$$\frac{\partial^4 \tilde{P}}{\partial \rho^4} + \frac{\partial^4 \tilde{P}}{\partial z^2 \partial \rho^2} - \beta_m \cos\theta \frac{\partial \tilde{P}}{\partial \rho} = 0 \tag{3.6}$$

where $\alpha = E^{\frac{1}{2}}/\sigma S$ and $\beta_m = 2\beta/E^{\frac{1}{4}}$ are $O(1)$. When $\beta_m \to 0$ (3.6) reduces, aside from a different notation, to the f-plane case, (equation (3.10), Merkine 1985). The appropriate boundary conditions for (3.4) are the Ekman compatibility conditions

$$\frac{\partial^2 \tilde{P}}{\partial \rho^2} = \pm \alpha \frac{\partial^3 \tilde{P}}{\partial \rho^2 \partial z} \quad \text{on } z = \tfrac{1}{2} \mp \tfrac{1}{2}, \tag{3.7}$$

the no-slip conditions

$$\tilde{P} = 0, \quad \frac{\partial \tilde{P}}{\partial \rho} = 0 \quad \text{on } \rho = 0, \tag{3.8}$$

and the matching condition

$$\tilde{P} \to \mp [a + b(z - \tfrac{1}{2})] r_0 \sin\theta \quad \text{on } \rho \to \infty. \tag{3.9}$$

The thermal wind relation

$$\frac{\partial \tilde{u}_\theta}{\partial z} = \frac{\partial \tilde{T}}{\partial \rho}, \tag{3.10}$$

which follows from (3.5), and (3.8) guarantee that to leading order the no-heat flux condition is automatically satisfied along the vertical wall. We note that (3.9) is not a regular Stewartson-matching condition since it is a mass flux condition and not a velocity-matching condition. (3.9) must be imposed if the $E^{\frac{1}{4}}$ layer is to accomplish its deflecting task. The strong jet-like tangential velocity which is $O(E^{-\frac{1}{4}})$ in the $E^{\frac{1}{4}}$ layer cannot be matched with the weaker $O(1)$ interior velocity that exists outside this layer. It follows that this strong velocity must decay to zero as $\rho \to \infty$. Our analysis is limited to obtaining an asymptotically consistent solution for the dominating field variables and for the wall shear stress and not for higher-order fields. For the same reasons we shall not discuss the inner $E^{\frac{3}{4}}$ layer whose dynamics is not explicitly influenced by β and whose contribution to the wall shear stress is of a higher order. The buoyancy layer is discussed thoroughly by Barcilon & Pedlosky (1967*b*) (see also Merkine 1985).

Equations (3.6)–(3.9) admit solutions of the form

$$f = \mathrm{e}^{-\lambda\rho} \sin(\gamma z + \phi), \tag{3.11}$$

provided

$$\tan\gamma = \frac{2\alpha\gamma}{\alpha^2\gamma^2 - 1}, \tag{3.12}$$

$$\phi = \sin^{-1}\left[\frac{\alpha\gamma}{(1+\alpha^2\gamma^2)^{\frac{1}{2}}}\right]$$

and

$$\lambda^3 - \alpha\gamma^2\lambda + \beta_m \cos\theta = 0. \tag{3.13}$$

It follows that the vertical structure of the eigenfunctions of the $E^{\frac{1}{4}}$ layer is not affected by β. The effect of the stratification parameter on these eigenfunctions and on the corresponding eigenvalues γ_n, is thoroughly discussed in Merkine (1985). (Note, however, the different notation, (3.12) corresponds to (3.16) and (3.17) of that paper with $1/\alpha$ corresponding to β and γ to χ.) The existence of the deflecting $E^{\frac{1}{4}}$ layer depends now on whether the roots of the cubic (3.13) yield a sufficient number of decaying exponentials such that all the radial boundary conditions can be satisfied. It turns out, as in Foster (1985), that a deflecting boundary layer exists only for $\cos\theta > 0$, regardless of the flow direction at infinity. From (3.12) and (3.13) we find that

$$\left.\begin{aligned} \gamma_n &\sim (n-1)\pi, \\ \lambda_{1n} &\sim \alpha^{\frac{1}{2}}\gamma_n, \\ \lambda_{2n} &\sim \frac{\beta_m \cos\theta}{\alpha\gamma_n^2}, \\ \lambda_{3n} &\sim -\alpha^{\frac{1}{2}}\gamma_n, \end{aligned}\right\} \tag{3.14}$$

as $n \to \infty$. λ_{3n} must be rejected and indeed for any n only two roots of the cubic are relevant. The roots of (3.13) are not always real. Two complex conjugate solutions exist for all

$$\gamma_n < \left(\frac{27\beta_m^2 \cos^2\theta}{4\alpha^3}\right)^{\frac{1}{6}}, \tag{3.15}$$

and in that case the real-λ root must be rejected. Complex roots indicate the existence of decaying Rossby waves within the $E^{\frac{1}{4}}$ layer. From the definition of β_m and α it follows that they increase in number as β or σS increase and disappear when $\theta \to \frac{1}{2}\pi$. It is important to observe that when $\beta_m \cos\theta \ll 1$ the estimate for λ_n given in (3.14) holds for all n. This indicates that as β_m decreases the deflecting layer widens up appreciably. In fact, it splits into two sublayers. The interior sublayer resembles the f-plane $E^{\frac{1}{4}}$ layer and the exterior sublayer becomes the stratified analogue of the Rossby layer of Foster. When $\theta = \frac{1}{2}\pi$, one exponential is lost and the present analysis is no longer applicable. The neighbourhood of $\theta = \frac{1}{2}\pi$ is treated in §3.2.

In view of the above discussion it is not difficult to show that the boundary-value problem (3.6)–(3.9) admits the following solution for $|\theta| < \frac{1}{2}\pi$:

$$\begin{aligned}\tilde{P} = {} & \mp r_0 \sin\theta[a+b(z-\tfrac{1}{2})] \pm \sin\theta \sum_{n=1}^{N} a_n \sin(\gamma_n z+\phi_n) \\ & \times [\cos(\lambda_n^{\mathrm{i}}\rho)+(\lambda_n^{\mathrm{r}}/\lambda_n^{\mathrm{i}})\sin(\lambda_n^{\mathrm{i}}\rho)]\,\mathrm{e}^{-\lambda_n^{\mathrm{r}}\rho} \\ & \pm \sin\theta \sum_{n=N+1}^{\infty} a_n \sin(\gamma_n z+\phi_n)(\lambda_{2n}\,\mathrm{e}^{-\lambda_{1n}\rho}-\lambda_{1n}\,\mathrm{e}^{-\lambda_{2n}\rho})/(\lambda_{2n}-\lambda_{1n}), \end{aligned} \tag{3.16}$$

$$a_n = 2r_0 \frac{2(a-\frac{1}{2}b)\gamma_n \sin(\phi_n+\frac{1}{2}\gamma_n)\sin(\frac{1}{2}\gamma_n) - b\gamma_n\cos(\phi_n+\gamma_n)+2b\sin(\frac{1}{2}\gamma_n)\cos(\phi_n+\frac{1}{2}\gamma_n)}{\gamma_n[\gamma_n-\cos(\gamma_n+2\phi_n)\sin\gamma_n]} \tag{3.17}$$

where N is the number of complex roots and $\lambda_n^{\mathrm{r}} = \mathrm{Re}\,[\lambda_n], \lambda_n^{\mathrm{i}} = \mathrm{I}_m[\lambda_n]$. The tangential velocity is given by

$$\begin{aligned}\tilde{u}_\theta = {} & \mp \sin\theta \sum_{n=1}^{N} a_n \sin(\gamma_n z+\phi_n)\,|\lambda_n|^2 \sin(\lambda_n^{\mathrm{i}}\rho)\,\mathrm{e}^{-\lambda_n^{\mathrm{r}}\rho}/\lambda_n^{\mathrm{i}} \\ & \mp \sin\theta \sum_{n=N+1}^{\infty} a_n \sin(\gamma_n z+\phi_n)\lambda_{1n}\lambda_{2n}(\mathrm{e}^{-\lambda_{1n}\rho}-\mathrm{e}^{-\lambda_{2n}\rho})/(\lambda_{2n}-\lambda_{1n}) \end{aligned} \tag{3.18}$$

and the wall shear stress by

$$\left.\frac{\partial\tilde{u}_\theta}{\partial\rho}\right|_{\rho=0} = \mp\sin\left\{\sum_{n=1}^{N} a_n|\lambda_n|^2\sin(\gamma_n z+\phi_n)+\sum_{n=N+1}^{\infty}\lambda_{1n}\lambda_{2n}\sin(\gamma_n z+\phi_n)\right\}. \tag{3.19}$$

It should be emphasized that the θ dependence enters not only through $\sin\theta$ but also through the dependence of λ_n on θ.

A prerequisite to the discussion of the corner region presented in §3.2 is the limiting form of the above solution for $\theta \to \frac{1}{2}\pi$. Equations (3.14) and (3.15) indicate that in this limit and also when $\theta \neq \frac{1}{2}\pi$ but $\beta_m \to 0$ the roots are real and that $\lambda_{2n} = o(\lambda_{1n})$. It follows that the width of the $E^{\frac{1}{4}}$ layer increases by a factor proportional to $(\beta_m\cos\theta)^{-1}$ and that the $O(1)$ mass flux is channelled now through this enlarged region. To obtain the structure of the solution in this wide exterior portion of the deflecting layer we define the slow variable

$$\bar{\rho} = \beta_m \cos\theta\rho, \tag{3.20}$$

and substitute it into (3.16). The desired expression is obtained when we consider the limit $\beta_m\cos\theta \to 0$ with $\bar{\rho} = O(1)$. The result is

$$P^{\mathrm{r}} = \mp r_0 \sin\theta[a+b(z-\tfrac{1}{2})] \pm \sin\theta \sum_{n=1}^{\infty} a_n \sin(\gamma_n z+\phi_n)\,\mathrm{e}^{-\bar{\rho}/\alpha\gamma_n^2}, \tag{3.21}$$

where

$$P^{\mathrm{r}} = \lim_{\beta_m \cos\theta \to 0} \tilde{P}(\bar{\rho}, z, \theta; \beta_m). \tag{3.22}$$

We note also that (3.21) corresponds to a balance between the last two terms of (3.6). Using the definition of a_n it follows that

$$\lim_{\bar{\rho}\to 0} P^{\mathrm{r}} = 0, \tag{3.23}$$

verifying indeed that the entire $O(1)$ mass flux flows in this enlarged portion of the vertical boundary layer. Thus, we have shown that P^{r} is the baroclinic analogue of the homogeneous Rossby layer of Foster (1985). The tangential velocity induced in the baroclinic Rossby layer does not satisfy the no-slip wall condition on $r = r_0$. This is accomplished by the inner part of the deflecting layer, which for $\beta_m \cos\theta \to 0$, is affected by β only through the matching condition for large ρ; otherwise, its structure is identical to that discussed by Merkine (1985). The inner limit as $\bar{\rho}\to 0$ of the tangential velocity in the Rossby layer is given by

$$u_\theta^{\mathrm{r}}(\bar{\rho} = 0) = \mp \sin\theta \sum_{n=1}^{\infty} \left(\frac{a_n}{\alpha\gamma_n^2}\right) \sin(\gamma_n z + \phi_n). \tag{3.24}$$

Considering the limit of (3.18) as $\beta_m \cos\theta \to 0$ at fixed ρ we obtain that

$$\frac{\tilde{u}_\theta}{\beta_m \cos\theta} \sim \mp \sin\theta \sum_{n=1}^{\infty} \left(\frac{a_n}{\alpha\gamma_n^2}\right)(1 - \mathrm{e}^{-\alpha^{\frac{1}{2}}\gamma_n \rho}) \sin(\gamma_n z + \phi_n), \tag{3.25}$$

which is the desired solution for this limiting form of the $E^{\frac{1}{4}}$ layer. (Note that $\tilde{u}_\theta = u_\theta^{\mathrm{r}} \beta_m \cos\theta$ and that (3.25) corresponds to a balance between the first two terms of (3.6).)

We can estimate now the importance of nonlinear effects. Here and in the subsequent sections we shall compare advection effects in the equations for vorticity and temperature with one of the dominating terms in each of these equations. The above solution indicates that diffusion of vorticity is $O(1)$ while buoyancy is $O(E^{\frac{1}{2}})$. Advection of vorticity is $O(\epsilon/E^{\frac{3}{4}})$ and advection of temperature is $O(\epsilon/E^{\frac{3}{4}})$. It follows that nonlinear effects can be ignored in the deflecting layer as long as $\epsilon \ll E^{\frac{3}{4}}$.

3.2. *The corner region*

The discussion of the previous subsection shows that a separate treatment is required for the neighbourhood of $r = r_0$ and $\theta = \frac{1}{2}\pi$. The widening of the deflecting layer as $\theta \to \frac{1}{2}\pi$ implies that the bulk of the corner region must be in geostrophic–hydrostatic balance. It can be shown that the equation for the leading-order pressure field, P^{cr}, in the exterior part of the corner region responsible for channelling the $O(1)$ mass flux is

$$\frac{\partial^4 P^{\mathrm{cr}}}{\partial z^2 \partial \mu_r^2} - \left(\frac{\beta_m}{\alpha}\right)\left[\chi \frac{\partial P^{\mathrm{cr}}}{\partial \mu_r} + \frac{1}{r_0}\frac{\partial P^{\mathrm{cr}}}{\partial \chi}\right] = 0 \quad \begin{matrix}(\mu_r = (r - r_0)/E^{\frac{1}{6}}),\\ (\theta = \frac{1}{2}\pi - E^{\frac{1}{12}}\chi),\end{matrix} \tag{3.26}$$

subject to the Ekman compatibility conditions (3.7) with μ_r replacing ρ. The solution of (3.26) must connect the solutions existing in the eastern and western sectors of the cylinder. Equation (3.26) is not easy to solve but it is possible to demonstrate that it admits solutions possessing the desired behaviour as $\chi \to \pm\infty$. Applying a technique similar to that employed by Foster we find that as $\chi \to \infty$

$$P^{\mathrm{cr}} = \mp r_0[a + b(z - \tfrac{1}{2})] \pm \sum_{n=1}^{\infty} a_n \sin(\gamma_n z + \phi_n)\, \mathrm{e}^{-\beta_m \eta/\alpha\gamma_n^2} + O(\chi^{-3}) \quad (\eta = \mu_r \chi), \tag{3.27}$$

and hence matching with (3.21) is possible. For $\chi < 0$ and large the desired solution of (3.26) consistent with the dynamics of the blocked region discussed next and capable of absorbing the $O(1)$ mass flux is

$$\left.\begin{aligned} P^{\mathrm{cr}} &= \mp\tfrac{1}{2}\sum_{n=1}^{\infty} a_n\left\{\mathrm{erf}\left[\left(\frac{\beta_m}{4\alpha\gamma_n^2}\right)^{\frac{1}{3}}\xi\right]+1\right\}\sin(\gamma_n z+\phi_n), \\ \xi &= \frac{\mu_r}{(-r_0\chi)^{\frac{1}{3}}}-\tfrac{1}{2}r_0^{\frac{1}{3}}(-\xi)^{\frac{2}{3}}. \end{aligned}\right\} \tag{3.28}$$

The tangential velocity in the outer part of the corner region does not satisfy the no-slip wall condition on $r = r_0$ and an inner layer of width $E^{\frac{1}{3}}$ is required. This inner layer is controlled by the same balance that yielded (3.25) and there is no need to pursue it any further.

Expression (3.28) implies that the tangential velocity induced at the wall by P^{cr} becomes exponentially small as $\chi\to-\infty$. The consequence is that the $E^{\frac{1}{3}}$ layer which is necessary at the corner region for imposing the no-slip wall condition on the solution of (3.26) disappears to leading order as $\chi\to-\infty$. We note also that for fixed μ_r and $\chi\to-\infty$ $\xi = O(|\chi|^{\frac{2}{3}})$ implying that the corner region widens up to $O(E^{\frac{1}{3}})$ *as* $\theta\to\frac{1}{2}\pi^-$. These last observations are important for our discussion of the free shear layer presented next.

In the $E^{\frac{1}{3}}$ layer of the corner region, vortex stretching is $O(E^{\frac{1}{3}})$ while buoyancy is $O(E^{\frac{2}{3}})$. Advection of vorticity is $O(\epsilon/E^{\frac{7}{12}})$ and advection of temperature is $O(\epsilon/E^{\frac{1}{3}})$. In the $E^{\frac{1}{3}}$ layer of the corner region, diffusion of vorticity is $O(E^{\frac{1}{12}})$ and buoyancy is $O(E^{\frac{7}{12}})$. Advection of vorticity is $O(\epsilon/E^{\frac{17}{24}})$ and advection of temperature is $O(\epsilon/E^{\frac{5}{24}})$. It follows that nonlinear effects appear first in the temperature equation of the $E^{\frac{1}{3}}$ layer and that they can be ignored uniformly in the corner region when $\epsilon \ll E^{\frac{11}{12}}$.

3.3. *The shear layer*

Our previous discussion showed that the deflecting boundary layer can exist only for $|\theta| < \frac{1}{2}\pi$. This implies that the region $r = O(1)$ bounded by $|\theta| > \frac{1}{2}\pi$ and $-r_0 < y < r_0$ must be blocked such that $|q| = o(1)$. This necessitates the existence of two intense jet-like regions at $y = \pm r_0$ which channel into or out of the corner region (depending on the flow direction at large distances from the cylinder) the $O(1)$ mass flux blocked by the cylinder. Otherwise, no reconciliation can exist with the imposed flow at $-r_0 < y < r_0$ and $x\to-\infty$. Following the observations made at the end of the previous subsection we assume that the leading-order dynamics in each of the two shear layers is in geostrophic–hydrostatic balance and rescale the corresponding field variables as follows:

$$\left.\begin{aligned} Y &= (\pm y - r_0)/E^{\frac{1}{3}}, \quad v = v^{\mathrm{s}}, \\ P &= P^{\mathrm{s}}, \quad w = E^{\frac{1}{3}}w^{\mathrm{s}}, \\ u &= u^{\mathrm{s}}/E^{\frac{1}{3}}, \quad T = T^{\mathrm{s}}, \end{aligned}\right\} \tag{3.29}$$

where the $\pm$ correspond to the shear layers at $y = \pm r_0$, respectively. (An $E^{\frac{1}{3}}$ layer with a balance similar to the $E^{\frac{1}{3}}$ layer of the corner region is possible also but it is not necessary for our leading-order motion.) Substitution of (3.29) into (2.1)–(2.4) leads to the following potential vorticity equation for the leading-order pressure field in each of the shear layers

$$P^{\mathrm{s}}_{YYzz} - (\beta_m/\alpha)\,P^{\mathrm{s}}_x = 0. \tag{3.30}$$

The appropriate boundary conditions are the Ekman compatibility conditions

$$P^s_{YY} = \pm\alpha P^s_{YYz} \quad \text{on } z = \tfrac{1}{2}\mp\tfrac{1}{2}, \tag{3.31}$$

and the mass flux constraints

$$\left.\begin{aligned} P^s &= \mp[a+b(z-\tfrac{1}{2})]\,r_0 \quad \text{as } Y\to\infty, \\ P^s &= 0 \qquad\qquad\quad \text{as } Y\to-\infty. \end{aligned}\right\} \tag{3.32}$$

In addition, the solution of (3.30) must match the corner-region solution at $\theta = \frac{1}{2}\pi^-$, namely (3.28). The solution for P^s is

$$P^s = \mp\tfrac{1}{2}\sum_{n=1}^{\infty} a_n\left\{\operatorname{erf}\left[\left(\frac{\beta_m}{2\alpha\gamma_n^2}\right)^{\frac{1}{2}}\tau\right]+1\right\}\sin(\gamma_n z+\phi_n) \quad \left(\tau = \frac{Y}{(-2x)^{\frac{1}{2}}}\right). \tag{3.33}$$

By expressing τ in terms of the corner-region variables it can be shown that (3.33) matches exactly (3.28).

The leading-order zonal velocity obtained from (3.33), namely

$$u^s = \pm\left(\frac{\beta_m}{4x\pi\alpha}\right)^{\frac{1}{2}}\sum_{n=1}^{\infty}\left(\frac{a_n}{\gamma_n}\right)\exp\left[-\left(\frac{\beta_m}{2\alpha\gamma_n^2}\right)\tau^2\right]\sin(\gamma_n z+\phi_n), \tag{3.34}$$

is a consequence of the $O(1)$ mass flux channelled through the shear layer. It does not smooth, however, the higher-order discontinuity associated with the zonal velocities

$$\left.\begin{aligned} u &= \pm[a+b(z-\tfrac{1}{2})] \quad \text{for } |y| > r_0, \\ u &= 0 \qquad\qquad\quad \text{for } |y| < r_0, \end{aligned}\right\} \tag{3.35}$$

existing outside the shear layer. To remove this discontinuity it is necessary to consider the $O(E^{\frac{1}{3}})$ correction to the pressure field which induces an $O(1)$ zonal velocity. Denoting this velocity by u_1^s we find that it is given by

$$u_1^s = \pm\left(\frac{1}{2r_0}\right)\sum_{n=1}^{\infty} a_n\left\{1-\tfrac{1}{2}\operatorname{erf}c\left[\left(\frac{\beta_m}{2\alpha\gamma_n^2}\right)^{\frac{1}{2}}\tau\right]\right\}\sin(\gamma_n z+\phi). \tag{3.36}$$

The shear layer spreads out as $x\to-\infty$, its width becoming comparable to r_0 when $-x = O(E^{-\frac{1}{4}})$. At this stage the jet's velocity, $u^s/E^{\frac{1}{3}}$, weakens to $O(1)$ and the expansion procedure fails since $u_1^s = O(1)$ also. The leading-order problem for the far field of the shear layer was formulated with $X = E^{\frac{1}{4}}x$ as the appropriate zonal lengthscale. On this scale the x extent of the cylinder shrinks to zero but in spite of this additional simplification no analytical solution could be obtained for the far-field region. It is comforting, however, that the flow behaviour in the far field of the shear layer has no consequence on the dynamically important intense flow that exists in the vicinity of the cylinder.

In the near field of the shear layer, vortex stretching is $O(E^{\frac{1}{4}})$, buoyancy is $O(E^{\frac{3}{4}})$, advection of vorticity is $O(\epsilon/E^{\frac{3}{8}})$ and advection of temperature is $O(\epsilon/E^{\frac{1}{8}})$. In the far field, vortex stretching is $O(E^{\frac{1}{3}})$, buoyancy is $O(E)$, advection of vorticity is $O(\epsilon E^{\frac{1}{4}})$ and advection of temperature is $O(\epsilon E^{\frac{1}{4}})$. It follows that nonlinear effect are negligible in the free shear layer provided $\epsilon \ll E^{\frac{1}{3}}$.

3.4. *Discussion*

A schematic representation of the vertical singular regions that arise from the presence of the cylinder is given in figure 1. Summarizing the nonlinear estimates stated above we find that advection of temperature in the Rossby-layer part of the

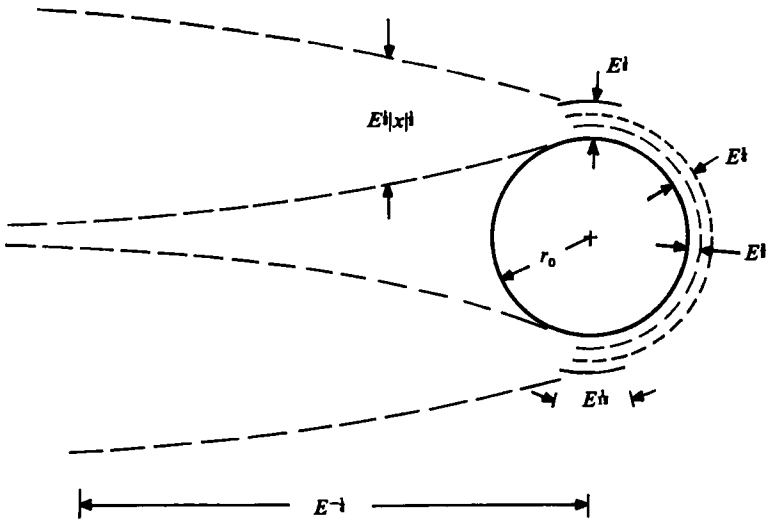

FIGURE 1. Schematic of the deflecting layer, the corner region and the free shear layer for moderate stratification.

corner region is the first nonlinearity to affect the dynamics as the Rossby number is progressively increased. It follows that nonlinear affects can be neglected everywhere provided that $\epsilon \ll E^{\frac{11}{12}}$. (The Ekman and the $E^{\frac{1}{3}}$ layers place less severe restrictions than those stated in the previous sections.) The Reynolds number can still be large as $E \to 0$ but it seems that it is much restricted compared to the f-plane case which requires that $Re \ll E^{-\frac{1}{2}}$ (Merkine 1985) or to the homogeneous case which, for $\beta = O(E^{\frac{1}{4}})$, requires that $Re \ll E^{-\frac{1}{4}}$, as can be inferred from Foster's parameter of nonlinearity. We note, however, that when $\epsilon = O(E^{\frac{11}{12}})$ the asymptotic solutions of the corner region must still be linear. Thus, unless we are interested in the details of the corner region we can relax the constraint on nonlinearity and replace it by the next in line which is imposed by the advection of temperature in the near field of the shear layer. The improvement is not significant, however, since it requires that $\epsilon \ll E^{\frac{11}{12}}$. We conclude that the deflecting layer becomes nonlinear at a much higher level of nonlinearity and long after other portions of the flow field have become nonlinear. In Foster's study, the corner region, the Rossby layer and the $E^{\frac{1}{3}}$ layer become nonlinear first and simultaneously.

We proceed now to study the effect of the free parameters on the dynamical behaviour of the system. We shall consider prograde flows only. Results for retrograde flows are obtained by reversing the flow direction. This applies also to the case of strong stratification discusssed in the next section and it is a consequence of the neglect of the advection terms.

The interpretation of the analytical results obtained above is simplified somewhat by considering first the shear layer. Figure 2 depicts the zonal velocity in the shear layer for a depth-independent flow at infinity which corresponds to $a = 1$ and $b = 0$ in (2.6). The vertical structure of the jet which is symmetric about $z = 0.5$ is nearly depth-independent and this seems to follow from the weak stratification since $\alpha = E^{\frac{1}{2}}/\sigma S = 10$. The striking feature of the figure is the effect of β_m. When it increases the shear layer narrows proportionally to $\beta_m^{-\frac{1}{2}}$ (see (3.34)) and the jet's velocity increases proportionally to $\beta_m^{\frac{1}{2}}$ as required by the $O(1)$ mass flux constraint.

Results for much stronger stratification, $\alpha = 0.1$, are shown in figure 3. The interior

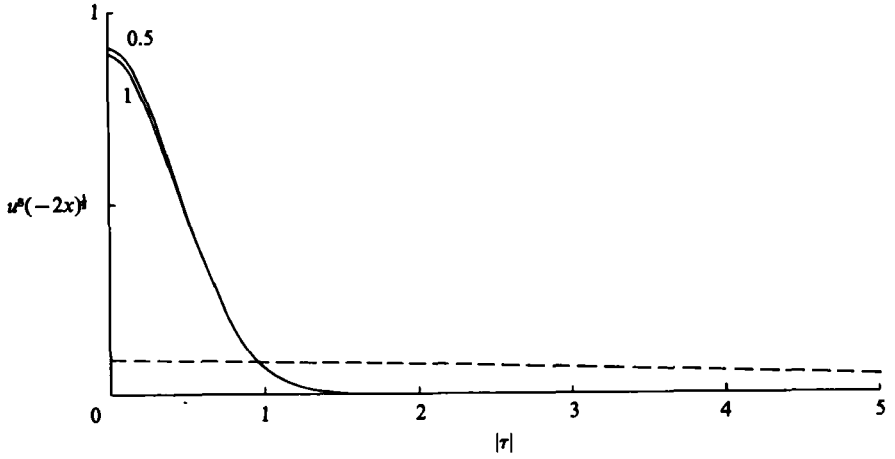

FIGURE 2. The meridional structure, multiplied by $(-2x)^{\frac{1}{2}}$, of the leading-order zonal velocity in the shear layer obtained from (3.34). Positive values correspond to motion in the direction of the flow at infinity. The figure is for height-independent zonal velocity at infinity ($a = 1$ and $b = 0$ in (2.6)) and the structure is symmetric about $z = 0.5$. The plots are for $\alpha = E^{\frac{1}{2}}/\sigma S = 10$. Full lines correspond to $\beta_m = 10$. The dashed line is for $\beta_m = 0.1$. The z-structure for $\beta_m = 0.1$ cannot be resolved on the plotted scale. The numbers denote the z-level.

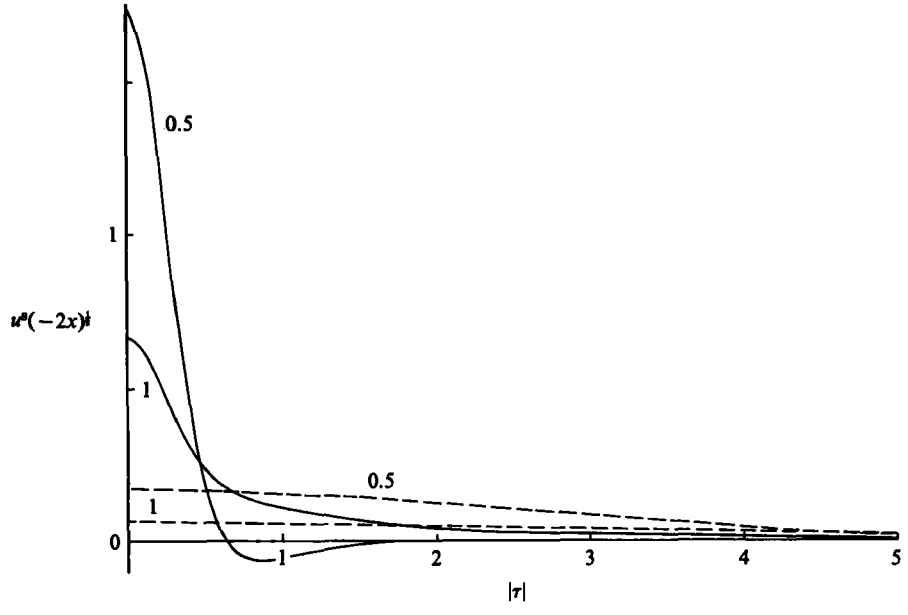

FIGURE 3. As in figure 2 but for $\alpha = 0.1$.

flow is barotropic but the jet is highly sheared in the vertical. The maximum velocity occurs at mid-height and it is accompanied by counter-flow regions existing along the jet's edges. These are new features not present in the homogeneous fluid of Foster (1985). They can be understood if we recognize that the vertical velocity induced by the Ekman layers is not a linear function of height and hence does not lead to a uniform vortex tube stretching in the vertical. The effect of the Ekman compatibility

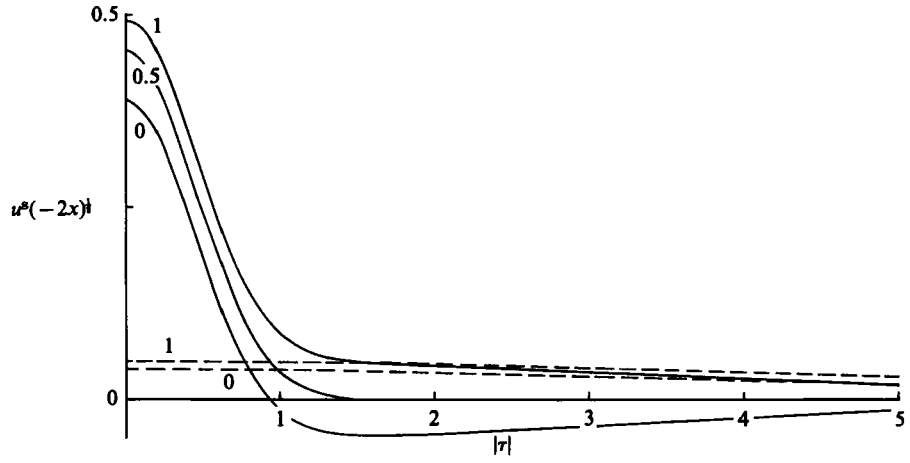

FIGURE 4. As in figure 2 but the flow at infinity vanishes on $z = 0$ and possesses unit vertical shear ($a = \frac{1}{2}$ and $b = 1$ in (2.6)).

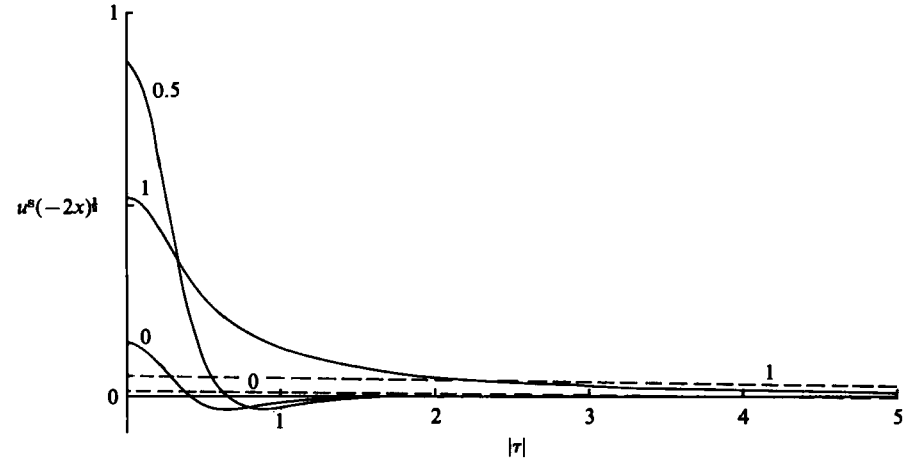

FIGURE 5. As in figure 4 but for $\alpha = 0.1$.

conditions (3.31), when expressed in terms of the horizontal shear of the zonal velocity, is to accentuate inward from the horizontal boundaries the horizontal shear that develops on $z = 0, 1$ because of the mass flux constraint. In the vicinity of $z = 0, 1$ the vertical increase in the horizontal shear and also in the central jet's velocity is proportional to $1/\alpha$ while (3.34) implies that the shear layer width is proportional to $\alpha^{\frac{1}{2}}$. (The eigenvalues γ_n are functions of α as well. Using their properties (Merkine 1985) it can be shown that the shear layer width is proportional to $\alpha^{\frac{1}{2}}$ for small α and becomes independent of α for large α.) It follows that as stratification increases (α decreases) the mass flux constraint cannot be satisfied unless counter-flow regions accompany the high-velocity regions.

We consider now a situation where the flow vanishes on $z = 0$ and possesses a unit vertical shear at infinity such that $a = \frac{1}{2}$ and $b = 1$ in (2.6). The zonal velocity of the shear layer is depicted in figures 4 and 5 for $\alpha = 10$ and $\alpha = 0.1$, respectively. When we contrast these figures with figures 1 and 2 we find two new features. First, the

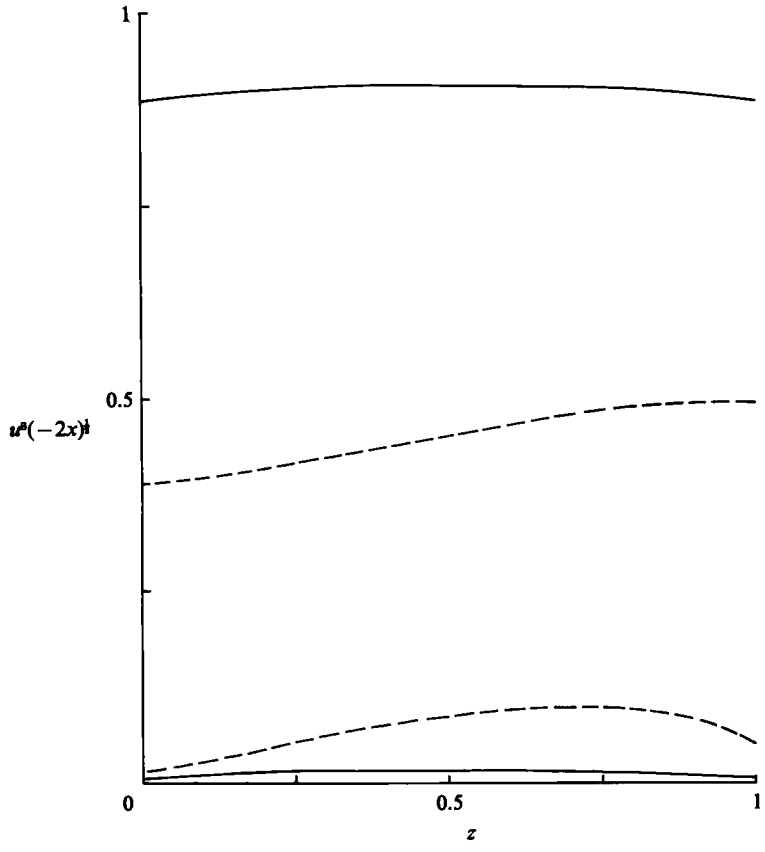

FIGURE 6. The vertical structure of the leading-order jet velocity multiplied by $(-2x)^{\frac{1}{2}}$ at the centre of the shear layer as a function of z for $\beta_m/\alpha = 1$. The two top lines correspond to $\beta_m = 10$ and $\alpha = 10$ and the two bottom lines correspond to $\beta_m = 0.1$ and $\alpha = 0.1$. The full lines are for $a = 1$ and $b = 0$. The dashed lines are for $a = \frac{1}{2}$ and $b = 1$.

jet's velocity does not vanish on $z = 0$ although the interior flow vanishes there. Secondly, figures 4 and 5 show that the jet's velocity on $z = 1$ is considerably smaller than the corresponding velocity depicted in figures 2 and 3, although the interior velocity on $z = 1$ is equal to 1 in both cases. The linear increase of the interior velocity with height requires that the $O(1)$ mass flux in the shear layer increases also linearly with height. This basic tendency is accompanied, as implied by the thermal wind relation, $T^s_Y = -u^s_z$, by a positive heat flux which attains its maximum at the jet's centre, decays to zero laterally and is a weak function of height. Considering the shear layer in the neighbourhood of $y = r_0$ we observe that the heat flux divergence is negative for $y > r_0$ and positive for $y < r_0$. The Ekman compatibility conditions (3.31) can be written as $u^s_Y = \pm\alpha(-T_Y)_Y$ where the upper/lower sign corresponds to the bottom/top level. It follows that the heat flux divergence generates on $z = 0$ negative horizontal shear for $y > r_0$ and positive horizontal shear for $y < r_0$. The consequence is a positive velocity in the vicinity of the jet's centre. The counter-flow regions existing along the edges of the jet are a consequence of the $O(1)$ mass flux which vanishes on $z = 0$. The effect of the heat flux is opposite on $z = 1$ and this reduces the jet's velocity when compared with the corresponding velocity depicted in figures 2

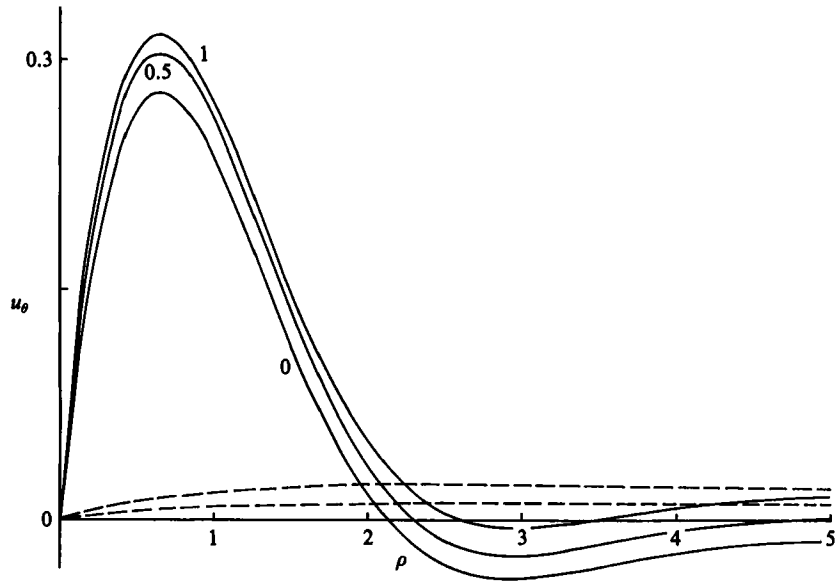

FIGURE 7. The radial structure of the leading-order tangential velocity (3.18) in the deflecting layer for $\alpha = E^{\frac{1}{2}}/\sigma S = 10$ and $\theta = \frac{1}{4}\pi$. Positive values correspond to motion in the direction of the flow at infinity. The full lines are for $\beta_m = 10$, $a = \frac{1}{2}$ and $b = 1$. The numbers denote the z-level. Results for $a = 1$ and $b = 0$ are not plotted. They are slightly less than twice the values for the curve plotted for $z = 0.5$. The dashed lines are for $\beta_m = 0.1$. The z-structure for $\beta_m = 0.1$ cannot be resolved on the plotted scale. The lower dashed line corresponds to $a = \frac{1}{2}$ and $b = 1$ and the upper dashed line corresponds to $a = 1$ and $b = 0$.

and 3 for the depth-independent interior flow. When the stratification is weak, the vertical structure of the jet is dominated by the vertical structure of the interior flow and the jet's velocity is a monotonic function of height, as observed in figure 4. When the stratification is strong, as in figure 5, the contribution of the barotropic part of the interior motion in conjunction with the Ekman compatibility conditions is to induce, similarly to the situation depicted in figure 3, a non-monotonic z-dependence of the jet's velocity. The vertical structure of the jet's velocity at the centre as a function of stratification for constant values of β_m/α is depicted in figure 6 for the two interior velocity profiles considered above.

Equation (3.30) can be interpreted as a balance that exists in the shear layer between relative vorticity creation by lateral motion on the β-plane and the removal of relative vorticity through vertical diffusion. The deflecting layer governed by (3.6) is narrower and horizontal diffusion of vorticity is as important as the two mechanisms just mentioned. Nevertheless, the structure of the deflecting layer responds to variations in β_m and α very similarly to the shear layer's response. The reason is the dynamical similarity that exists between the vertical wall and the blocked region in terms of how they affect the leading-order motion adjacent to them. Both act to reduce it, and the asociated heat flux, to zero. Figures 7 and 8 which depict at $\theta = \frac{1}{4}\pi$ the structure of the deflecting layer's streamwise velocity exhibit all the features discussed earlier. The variation of the structure with θ at fixed β_m can be interpreted by varying β_m at fixed θ since the dependence on θ is parametric and it is combined with β_m into the parameter $\beta_m \cos\theta$ that appears in (3.6).

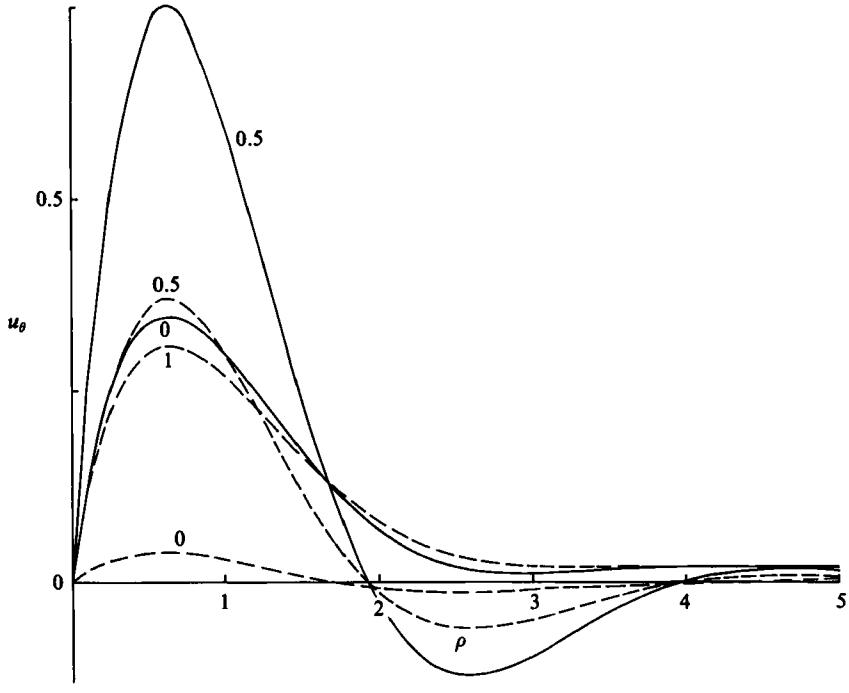

FIGURE 8. The radial structure of the leading-order tangential velocity (3.18) in the deflecting layer at $\theta = \frac{1}{4}\pi$ for $\alpha = E^{\frac{1}{2}}/\sigma S = 0.1$ and $\beta_m = 10$. Positive values correspond to motion in the direction of the flow at infinity. Full lines correspond now to $a = 1$ and $b = 0$ (the structure is symmetric about $z = 0.5$) and dashed lines to $a = \frac{1}{2}$ and $b = 1$. The numbers denote the z-level. Results for $\beta_m = 0.1$ are not plotted. They correspond to small-amplitude decaying long waves.

4. Strong β, strong stratification $E \ll \beta \ll 1, \sigma S = O(1)$

When the flow is in geostrophic–hydrostatic balance to leading order (see (3.2)) the quasi-geostrophic vorticity equation is

$$\epsilon \boldsymbol{q}^0 \cdot \nabla \nabla_{\mathrm{H}}^2 P^0 - \frac{\partial w}{\partial z} + \beta \frac{\partial P^0}{\partial x} = \tfrac{1}{2} E \nabla^2 \nabla_{\mathrm{H}}^2 P^0,$$

while the leading-order equation for the temperature field becomes

$$\sigma \epsilon \boldsymbol{q}^0 \cdot \nabla P_z^0 + \sigma S w = \tfrac{1}{2} E \nabla^2 P_z^0.$$

Note that when $\sigma S = O(1)$ and $\epsilon \ll E, w = O(E)$ outside thin vertical layers. Eliminating w between the last two equations yields the following balance for the quasi-geostrophic potential vorticity

$$\epsilon \boldsymbol{q}^0 \cdot \nabla \left(\nabla_{\mathrm{H}}^2 P^0 + \frac{1}{S} P_{zz}^0 \right) + \beta \frac{\partial P^0}{\partial x} = \tfrac{1}{2} E \nabla^2 \left(\nabla_{\mathrm{H}}^2 + \frac{1}{\sigma S} \frac{\partial^2}{\partial z^2} \right) P^0.$$

Thus, it seems that advection is negligible compared to diffusion as long as $\epsilon \ll E$ or when the Reynolds number is small. This constraint remains in effect as long as $\beta = O(E)$. The results of this section show that the balance

$$\nabla^2 \left(\nabla_{\mathrm{H}}^2 + \frac{1}{\sigma S} \frac{\partial^2}{\partial z^2} \right) P^0 - \beta_{\mathrm{s}} \frac{\partial P^0}{\partial x} = 0 \quad (\beta_{\mathrm{s}} = 2\beta/E), \tag{4.1}$$

is valid for properly restricted large Reynolds numbers provided β is large compared to E. The reason is the consequent smallness of

$$\boldsymbol{q}^0 \cdot \boldsymbol{\nabla}\left(\nabla_{\mathrm{H}}^2 P^0 + \frac{1}{S} P^0_{zz}\right).$$

(4.1) is supplemented by the boundary conditions

$$\nabla_{\mathrm{H}}^2 P^0 = 0 \quad \text{on } z = 0, 1, \tag{4.2}$$

$$P^0_{zz} = 0 \quad \text{on } z = 0, 1, \tag{4.3}$$

$$\frac{\partial P^0}{\partial r} = \frac{\partial P^0}{\partial \theta} = 0 \quad \text{on } r = r_0, \tag{4.4}$$

$$P^0 = -U(z)\, y \quad \text{as } r \to \infty; \quad U(z) = \pm[a + b(z - \tfrac{1}{2})], \tag{4.5}$$

whose derivation follows from Barcilon & Pedlosky (1967*a*) and is given in Merkine (1985). To summarize, the boundary-value problem given by (4.1)–(4.5) is appropriate for the range $0 < \beta \ll 1$ however, when $\beta = O(E)$ it is required that $Re \ll 1$. This restriction on Re can be relaxed when $\beta \gg E$ and the exact constraint on Re will be stated subsequently. The smallness of β is required for the validity of the β-plane approximation.

For the reasons outlined in § 2 we limit our investigation to the strong-β case such that $\beta_{\mathrm{s}} \gg 1$ and extend the analysis of Foster (1985) to strongly stratified flows. Since the analysis presented in this section is similar to the analysis of the previous section it suffices to state the results. (Interested readers can obtain from the Editorial office more detailed derivation of the solutions stated below.) Thus away from singular surfaces the interior constraint (3.3) must be satisfied to leading order. Along the eastern sector of the cylinder a deflecting boundary layer of width $(E/\beta)^{\frac{1}{3}}$ exists. It is governed by the equation

$$\frac{\partial^4 \tilde{P}}{\partial \rho^4} - \cos\theta \frac{\partial \tilde{P}}{\partial \rho} = 0, \tag{4.6}$$

which is a balance between the creation of vorticity by the meridional motion on the β-plane and its removal by horizontal diffusion. This is the balance that exists in Munk's western boundary layer (Munk 1950). Here $\tilde{P}$ is the leading-order pressure field and $\rho = (r - r_0)\beta_{\mathrm{s}}^{\frac{1}{3}}$ is the boundary-layer coordinate. It follows that

$$\tilde{P} = -U(z) r_0 \sin\theta \left\{1 - \left(\frac{2}{3^{\frac{1}{2}}}\right) \exp\left[-(\cos\theta)^{\frac{1}{3}} \tfrac{1}{2}\rho\right] \cos\left[\tfrac{1}{2}3^{\frac{1}{2}}(\cos\theta)^{\frac{1}{3}}\rho - \tfrac{1}{6}\pi\right]\right\}. \tag{4.7}$$

The compatibility of (4.7) with the quasi-geostrophic dynamics requires that $E^{\frac{1}{3}}\beta_{\mathrm{s}}^{\frac{1}{3}} \ll 1$ and this is assured since $E \ll \beta \ll 1$. The leading-order tangential velocity associated with this pressure field and hence with the boundary layer $O(1)$ mass flux is

$$\tilde{u}_\theta = -(2/3^{\frac{1}{2}})\, U(z) r_0 \sin\theta (\cos\theta)^{\frac{1}{3}} \sin\left[\tfrac{1}{2}3^{\frac{1}{2}}(\cos\theta)^{\frac{1}{3}}\rho\right] \exp\left[-(\cos\theta)^{\frac{1}{3}}\tfrac{1}{2}\rho\right]. \tag{4.8}$$

We observe that the z-dependence is parametric and it is impressed by the vertical structure at infinity. This highly two-dimensional structure prevails also in the corner region and in the shear-layer region. It can be shown that nonlinear effects can be ignored in the deflecting layer as long as $\epsilon \ll E^{\frac{2}{3}}\beta^{\frac{1}{3}}$.

The leading-order pressure field, P^{s}, in the shear layer in the vicinity of the cylinder is governed by the equation

$$\frac{\partial^4 P^{\mathrm{s}}}{\partial Y^4} - \frac{\partial P^{\mathrm{s}}}{\partial x} = 0 \quad (Y = (\pm y - r_0)\beta_{\mathrm{s}}^{\frac{1}{3}}), \tag{4.9}$$

subject to the asymptotic mass flux constraints

$$\left.\begin{aligned} P^{\mathrm{s}} &= -U(z)\,r_0 \quad \text{as } Y\to\infty, \\ P^{\mathrm{s}} &= 0 \quad \text{as } Y\to-\infty, \end{aligned}\right\} \tag{4.10}$$

and the initial condition

$$P^{\mathrm{s}} = -U(z)\,r_0\,H(Y), \tag{4.11}$$

where $H(Y)$ is Heaviside's step function. The solution for P^{s} is

$$P^{\mathrm{s}} = -\tfrac{1}{2}U(z)\,r_0\left[\frac{2}{\pi}\int_0^\infty \mathrm{d}L L^{-1}\sin(L\tau)\exp(-L^4)+1\right] \quad (\tau = Y/(-x)^{\frac{1}{4}}), \tag{4.12}$$

while the leading-order streamwise velocity is given by

$$u^{\mathrm{s}} = \frac{r_0\,U(z)}{\pi(-x)^{\frac{1}{4}}}\int_0^\infty \mathrm{d}L\cos(L\tau)\exp(-L^4). \tag{4.13}$$

The leading-order zonal velocity u^{s} is a consequence of the $O(1)$ mass flux channelled through the shear layer and as such it cannot smooth out the higher-order discontinuity associated with the $O(1)$ velocity jump across the shear layer. This weaker discontinuity is removed by the $O(\beta_{\mathrm{s}}^{-\frac{1}{4}})$ contribution to the pressure field. Denoting the corresponding $O(1)$ zonal velocity by u_1^{s} it can be shown that

$$u_1^{\mathrm{s}} = \tfrac{1}{2}U(z)\left[\frac{2}{\pi}\int_0^\infty \mathrm{d}L L^{-1}\sin(L\tau)\exp(-L^4)+1\right]. \tag{4.14}$$

The deflecting layer and the shear layer exchange the $O(1)$ mass flux through a corner region whose limit equation for the leading-order pressure field P^{c} is

$$\frac{\partial^4 P^{\mathrm{c}}}{\partial\mu^4} - \chi\frac{\partial P^{\mathrm{c}}}{\partial\mu} - \frac{1}{r_0}\frac{\partial P^{\mathrm{c}}}{\partial\chi} = 0 \quad (\mu = (r-r_0)\beta_{\mathrm{s}}^{\frac{2}{3}},\quad \theta = \tfrac{1}{2}\pi - \chi/\beta_{\mathrm{s}}^{\frac{1}{3}}) \tag{4.15}$$

P^{c} satisfying the appropriate boundary conditions has the following asymptotic solutions:

$$\left.\begin{aligned} P^{\mathrm{c}} &\sim -U(z)\,r_0\left\{1-\left(\frac{2}{3^{\frac{1}{2}}}\right)\exp[-\tfrac{1}{2}\eta]\cos[\tfrac{1}{2}3^{\frac{1}{2}}\eta-\tfrac{1}{6}\pi]\right\} \quad \text{as } \chi\to\infty;\quad \eta = \chi^{\frac{1}{3}}\mu, \\ P^{\mathrm{c}} &\sim -U(z)\,r_0\,G(\xi);\quad \xi = \frac{\tfrac{1}{2}(\mu - r_0(-\chi)^2)}{(-r_0\chi)^{\frac{1}{4}}} \quad \text{as } \chi\to-\infty;\quad G_{\xi\xi\xi\xi} - \tfrac{1}{4}\xi G_\xi = 0, \end{aligned}\right\} \tag{4.16}$$

and hence it merges smoothly with the deflecting layer and with the shear layer. (Note that the equation for P^{s} expressed in terms of the similarity variable τ is $P^{\mathrm{s}}_{\tau\tau\tau\tau} - \frac{1}{4}\tau P^{\mathrm{s}}_\tau = 0$.) Nonlinear effects can be ignored in the corner region when $\epsilon \ll E^{\frac{4}{7}}\beta^{\frac{1}{7}}$.

When $-x = O(\beta_{\mathrm{s}})\,u^{\mathrm{s}}$ and u_1^{s} become comparable and the asymptotic expansion is no longer valid. When this happens lateral diffusion of vorticity has weakened to the level where vorticity generation by the now $O(E)$ vertical velocity can no longer be neglected and the z-dependence of the solution is no longer parametric. The structure of the flow in the far field of the shear layer is highly complicated but as it is not important dynamically it will not be presented here. Estimation of nonlinear effects in the shear layer leads to the conclusion that they can be safely ignored in the near field when $\epsilon \ll \beta^{\frac{1}{2}}E^{\frac{3}{4}}$ and in the far field when $\epsilon \ll \beta$. It follows that the shear layer becomes nonlinear first in the near field.

A schematic representation of the vertical singular regions that arise for the range of parameters considered in this section is shown in figure 9. Summarizing the

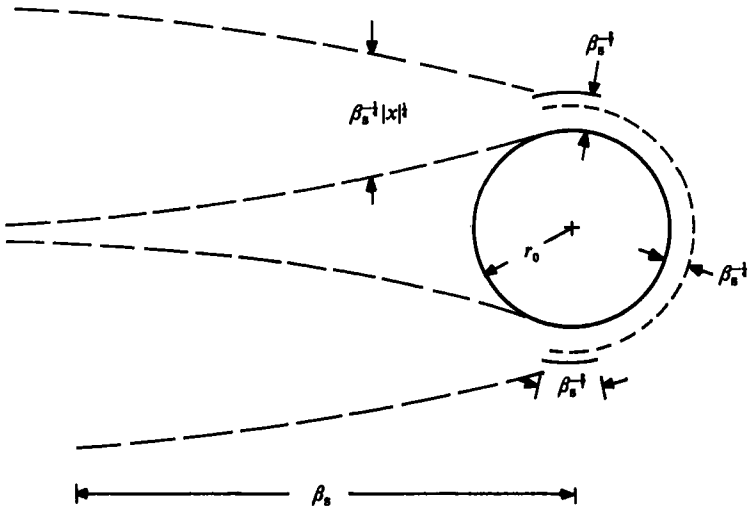

FIGURE 9. Schematic of the deflecting layer, the corner region and the free shear layer for strong stratification.

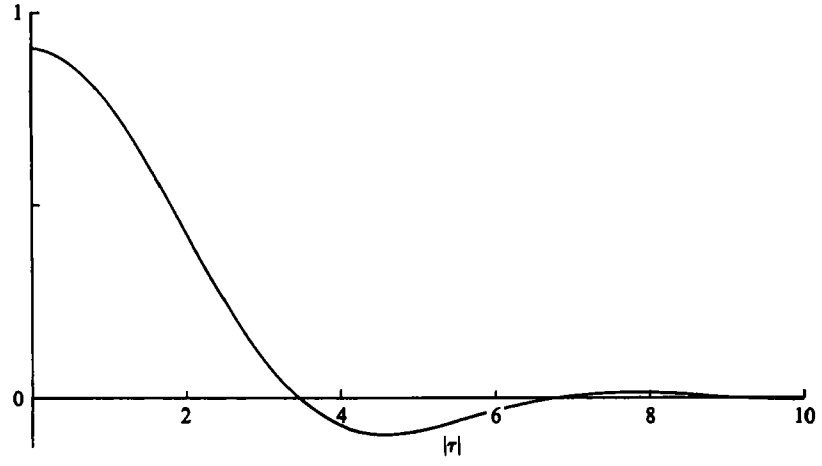

FIGURE 10. The integral in (4.13) as a function of the similarity variable τ defined in (4.12). It determines the meridional structure of the leading-order zonal velocity in the free shear layer for strong stratification. Positive values correspond to motion in the direction of the flow at infinity.

nonlinear estimates stated above we find that nonlinearity appears first in the corner region. The free shear layer is affected next and only then the deflecting layer. (The Ekman layer places less severe restrictions on nonlinearity.) It follows that nonlinear effects can be neglected everywhere when $\epsilon \ll E^{\frac{4}{3}}\beta^{\frac{1}{3}}$ or $Re \ll \beta^{\frac{1}{3}}/E^{\frac{1}{3}}$. In the corresponding f-plane case and also when $\beta_s = O(1)$ nonlinear effects can be neglected when $\epsilon \ll E$ or $Re \ll 1$ and these restrictions stem from the nonlinear advection of temperature. The dramatic increase in the allowable Reynolds number for the linear analysis to remain valid follows from the strong-β strong-stratification combination. In this parameter regime the vorticity induced in the vertical singular surfaces by rising isopycnal surfaces is insignificant compared to the production of vorticity by the meridional motion while production is balanced by horizontal diffusion. The

consequence is the parametric z-dependence of the leading-order motion whose vertical structure is that of the flow at infinity. This parametric dependence is sufficient to nullify the nonlinear advection of the temperature and to raise the upper bound imposed on the Reynolds number.

The leading-order vorticity balance in the singular regions forces short decaying Rossby waves which manifest themselves as counter-flows in the deflecting layer (see (4.6)) and in the free shear layer (see figure 10). In Foster's shear layer where the balance is as in the western boundary layer of Stommel (1948), i.e. between the production of vorticity by the meridional motion and its dissipation by Ekman suction, no counter-currents exist.

5. Conclusion

We have made a linear analysis of stratified rotating flow past a circular cylinder on a β-plane thus supplementing the analogue f-plane study of Merkine (1985). The mathematical complications introduced by the variability of the Coriolis parameter could be tackled analytically only when the production of relative vorticity by the meridional motion was allowed to dominate the dynamics. In that case the bulk of the flow field was constrained to follow geostrophic contours, i.e constant y-lines in our case. This is enough to alter the dynamics significantly compared to the f-plane configuration since the geometric constraint imposed by the cylinder is felt at large distances to the west of the cylinder while the opposite occurs in the east. We have purposely refrained from using the terminology 'upstream' and 'downstream' since the east–west asymmetry imposed by the β-effect in the linear regime is invariant to the flow direction at infinity. Retrograde flow solutions can be obtained from prograde flow solutions by merely reversing the flow direction. This conclusion will not remain uniformly valid when advection terms are allowed to become important somewhere in the flow field. Although stratification could not modify drastically the basic features obtained by Foster (1985) in his consideration of homogeneous fluid, new dynamical features were discovered. The most striking one is the appearance of counter-flows. In that sense the subtle consequences of stratification described in Merkine (1985) reappear here.

The experiments of Boyer (1970) and Boyer & Davies (1982) as well as the more recent ones by Boyer & Kmetz (1983) and Boyer *et al.* (1984) concentrated on the dynamical aspects of the shed vortices. This is partly because of the possible importance of such vortices in geophysical applications and partly because of the technical difficulties involved in boundary-layer measurements, in particular in rotating systems. Vortex formation is related to the dynamics of the vertical boundary layer through the phenomenon of separation, and the nonlinear studies of Walker & Stewartson (1972), Merkine & Solan (1979), Merkine (1980), Foster (1985), Brevdo & Merkine (1985), and Merkine & Brevdo (1986) were able to explain certain features related to the appearance of vortices in rotating homogeneous fluids. No such studies are available for continuously stratified systems. However, since much insight into the stratified flow response has been gained by the linear analysis of the f-plane and β-plane dynamics we feel that nonlinear effects should be pursued next. It is straightforward to formulate the nonlinear dynamics of the vertical singular regions but the solution of the problem is a formidable task not only in the strong β-limit where the corner region becomes nonlinear first but also in the f-plane case as can be seen from the nonlinear problem for moderate stratification stated by Merkine (1985). It is our intention to consider such problems in the future.

Finally it should be pointed out that the effect of β is simulated in the laboratory through the tilt of a horizontal bounding surface by a small angle β. In stratified fluids the Taylor–Proudman theorem does not hold and the effect of the tilt cannot appear explicitly in the potential vorticity equation as it does for a homogeneous fluid or when the motion is on a sphere. However, when the tilt is sufficiently strong compared to $E^{\frac{1}{2}}$, strong jets and blocking should develop at least next to the tilted plane, as can be inferred from an estimate of the vertical velocity induced by the tilt and the constraints imposed on it by the Ekman suction and buoyancy. It seems desirable that such experiments be carried out.

A suitable set-up is the 2.4 m long tow tank used in the recent rotating stratified experiments of Boyer *et al.* (1987) who investigated the flow past three-dimensional tall obstacles. f-plane geometry was considered but β-plane effects can presumably be introduced by tilting the top and bottom bounding surfaces as done in the experiments of Boyer & Davies (1982). In the rotating stratified experiments the tow tank was filled with linearly stratified salt-water fluid. Because of the large ratio of kinematic viscosity to salt diffusivity the equivalent of σS assumed values of a few thousand and this places the experiments in the strong stratification category. The range of E was about 10^{-4} and the smallest Rossby number was about 0.05. In terms of the present analysis and that of Merkine (1985) the flow response was strongly nonlinear. (The Reynolds numbers was in the hundreds.) It follows that in order to be able to compare the linear analysis with the experiments using the above fluid the towing velocity must be greatly reduced from its typical value of 1 cm/s if the rotation rate is kept at its present range of 0.25–0.50 s^{-1}.

This research has been sponsored in part by the Air Force Office of Scientific Research, under Grant AFOSR-83-0069.

REFERENCES

Barcilon, V. & Pedlosky, J. 1967*a* Linear theory of rotating stratified fluid motions. *J. Fluid Mech.* **29**, 1–16.

Barcilon, V. & Pedlosky, J. 1967*b* A unified linear theory of homogeneous and stratified rotating fluids. *J. Fluid Mech.* **29**, 609–621.

Boyer, D. L. 1970 Flow past a right circular cylinder in a rotating frame. *Trans. ASME* D: *J. Basic Engng* **92**, 430–436.

Boyer, D. L. & Davies, P. A. 1982 Flow past a circular cylinder on a β-plane. *Phil. Trans. R. Soc. Lond.* A **306**, 533–556.

Boyer, D. L. & Kmetz, M. L. 1983 Vortex shedding in rotating flows. *Geophys. Astrophys. Fluid Dyn.* **26**, 51–83.

Boyer, D. L., Kmetz, M. L., Smithers, L., Chabert d'Hiers, G. & Didelle, H. 1984 Rotating open channel flow past right circular cylinders. *Geophys. Astrophys. Fluid Dyn.* **30**, 271–304.

Boyer, D. L., Davies, P. A., Holland, W. R., Biolley, F. & Honji, H. 1987 Stratified rotating flow over and around isolated three-dimensional topography. *Phil. Trans. R. Soc. Lond.* A **322**, 213–241.

Brevdo, L. & Merkine, L. 1985 Boundary layer separation of a two-layer rotating flow on an f-plane. *Proc. R. Soc. Lond.* A **400**, 75–95.

Foster, M. R. 1985 Delayed separation in eastward rotating flow on a beta plane. *J. Fluid Mech.* **155**, 59–75.

Merkine, L. 1980 Flow separation on a β plane. *J. Fluid Mech.* **99**, 399–409.

Merkine, L. 1985 A linear analysis of rotating stratified flow past a circular cylinder on an f-plane. *J. Fluid Mech.* **157**, 501–518.

MERKINE, L. & BREVDO, L. 1986 Boundary-layer separation of a two-layer rotating flow on a β-plane. *J. Fluid Mech.* **167**, 31–48.

MERKINE, L. & SOLAN, A. 1979 The separation of flow past a cylinder in a rotating system. *J. Fluid Mech.* **92**, 381–392.

MUNK, W. H. 1950 On the wind driven ocean circulation. *J. Met.* **7**, 79–93.

STOMMEL, H. 1948 The westward intensification of wind-driven ocean currents. *Trans. Am. Geophys. Union* **99**, 202–206.

WALKER, J. D. & STEWARTSON, K. 1972 The flow past a circular cylinder in a rotating frame. *Z. angew Math. Phys.* **23**, 745–752.